Fiber Optic Communications Using Liquid-Crystal-Based Fourier Optical Spectrum Analyzer without Moving Parts

Kashish Bhargava[1], Vivek Saxena[2], Anuj Jain[3]

[1]*M.Tech Scholar, ECE Department, Bhagwant University, Rajasthan, India*
[2]*Assistant Professor, ECE Department, Bhagwant University, Rajasthan, India*
[3]*Assistant Professor, ECE Department, Bhagwant University, Rajasthan, India*

ABSTRACT

We propose and demonstrate a liquid-crystal (LC)-based Fourier optical spectrum analyzer (FOSA). The FOSA consists of a birefringent filter array with an embedded LC phase modulator. The LC phase modulator is used to control the phase difference between two orthogonally polarized beams to avoid mechanical movement in conventional Fourier transform spectrometers. The detailed operation principle of this FOSA is described. A single-LC-based 6-stage FOSA is experimentally demonstrated, and the results obtained using such a FOSA show good agreement with the results measured using a reference spectrometer. We propose a liquid crystal (LC)-based cost-effective Fourier optical spectrum analyzer (FOSA) without moving parts. Unlike normal spectrometers, the LC FOSA retrieves the spectrum's Fourier coefficients instead of the direct spectrum measurement by changing different LC states in a number of stages. Besides the common applications, the LC FOSA can precisely read and recover the envelope of a dense wavelength-division-multiplexing spectrum to act as a spectral monitor and then work with a gain-flattening device to control the optical network instantly and dynamically.

Keyword : - *LC, FOSA, LC FOSA, Stage, Cost, Fourier transform* .

1. INTRODUCTION

The continuously increasing data capacity requirements in telecommunications have led to an increased demand for high speed optical devices for optical communications systems. Highly compact, non-mechanical and high speed optical devices are in a great demand, particularly for the next-generation dynamically reconfigurable networks. LCs have traditionally been primarily used in LC display (LCD) technologies. In addition to LCD devices, LC materials are considered potentially suitable for tunable photonic device applications. Unlike LC display devices, photonic devices for optical communications applications operate in the infrared range of wavelengths. LCs with their low absorption in the infrared region and large electro-optical response are considered an important material for tunable optical devices in optical communications. With easy tunability achievable by thermal and electrical means extensive research has been undertaken so far to exploit this advantage of LCs for various applications in optical communications. LCs have been employed in bulk optical device applications in optical communications. The use of LC in bulk devices has the advantage of ease of fabrication and allows for precise control of the design characteristics of the device due to the fact that the LC cells can easily made with appropriate thicknesses and suitable shapes. However due to the presence of bulk
optical components such devices have high coupling losses and have practical issues with integration with fiber, which reduces their attractiveness in fiber based applications. As an alternative to a bulk approach, LC based devices have been implemented with integrated optics and waveguide based approaches. In most of these demonstrations of LCs based tunable devices, LCs are employed in bulk configurations, which normally are in the form of a LC cell functioning as a variable phase retarder. For most of the device applications in optical communications, an all-fiber

device configuration is often preferred for easy integration with the interconnecting fibers within an optical communication network.

2. LIQUID CRYSTAL

Liquid crystal (LC) science and technology now underpins a wide variety of products, from large industrial displays to a wide array of consumer electronics in homes and offices. Non-display applications of LCs in optical communication, nonlinear optics, data/signal/image processing and optical sensing are also receiving increased attention. Due to their unique crystalline phase characterized by the partial order of their constituent molecules along with physical fluidity, LCs can be easily incorporated into desired configurations for a variety of device applications. The large anisotropy of LCs, allows for realisation of external control of the optical properties of LC based devices, which makes LC materials suited for implementing tunable photonic devices for both optical communications and optical sensing systems. The increasing demand for very high data capacity has meant that all-fiber fast tunable devices are in high demand in optical communications systems.

3. LIQUID CRYSTAL INFILTRATED PHOTONIC CRYSTAL FIBER FOR APPLICATIONS IN OPTICAL COMMUNICATION SYSTEMS

Electrical tuning of the photonic bandgap transmission properties of a liquid crystal infiltrated PCF is experimentally studied in this thesis for applications in optical communications systems. The infiltration of LCs into PCFs allows for the electrical tunability of the photonic bandgaps of the fiber in a wavelength range from 1500 nm – 1600 nm, which allows for the implementation of a variable optical attenuator and an all-fiber tunable notch filter, suited for various applications in optical communication systems and potentially in optical sensing. From these studies the following conclusions were drawn:

• Liquid crystal infiltrated photonic crystal fiber is found to be a suitable technology for the implementation of a variety of all-fiber tunable photonic devices for optical communications, with the important advantage of simple fiber interfacing.

• A nematic LC infiltrated PCF operating on the principle of photonic bandgap guidance was demonstrated as an all-fiber electrically controlled broadband variable optical attenuator.

The LCPCF device exhibits ~ 40 dB attenuation between its high and low states and has a linear attenuation response with applied voltage. The electrical tuning of photonic bandgaps of a smectic LC infiltrated PCF was demonstrated in the wavelength range of 1500 nm – 1600 nm for application as an all-fiber tunable notch filter.

4. LIQUID FOURIER TRANSFORM SPECTROMETER

Traditional Fourier transform spectrometers possess two major advantages over grating, prism, and circular variable filter (CVF) spectrometers. One is the time-multiplexing effect. The Michelson interferometer's single detector views all the wavelengths (within the sensor passband) simultaneously throughout the entire measurement. This effectively lets the detector collect data on each wavelength for the entire measurement time, measuring more photons and therefore, results in higher signal-to-noise ratio, at best for situations where the sou/rce is stable. The other is the throughout advantages since the FTS does not need spatial filters (e.g. slit) in the optical light path. Fourier transform spectroscopy is a measurement technique whereby spectra are collected based on measurements of the coherence of a radiative source, using time-domain or space-domain measurements of the electromagnetic radiation or other type of radiation. It can be applied to a variety of types of spectroscopy including optical spectroscopy, infrared spectroscopy (FTIR, FT-NIRS), nuclear magnetic resonance (NMR) and magnetic resonance spectroscopic imaging (MRSI),[1] mass spectrometry and electron spin resonance spectroscopy.

5. LIQUID CRYSTAL PHASE MODULATOR ARRAY BASED ADAPTIVE ATTENUATOR

This is a transmission type adaptive attenuator. A plane wave is incident upon the liquid crystal based phase modulator array. Refractive index of each unit of the array can be controlled electronically. The light through each unit is deemed as one beam. The beams that go through the array will interfere with each other after the second focus lens. By changing the refractive index of each unit of the array so as to allocate the phase difference, we can use a computer to arbitrarily allocate $\{T\}$ among the beams. Group k unit into m groups. Among each group, $\Delta T=0$

{*A*(*T*)} allocation is achieved. allocation is achieved. When the number of unit is large, energy allocation and phase allocation can be changed individually. The system deployment is plotted in Figure 1.1.

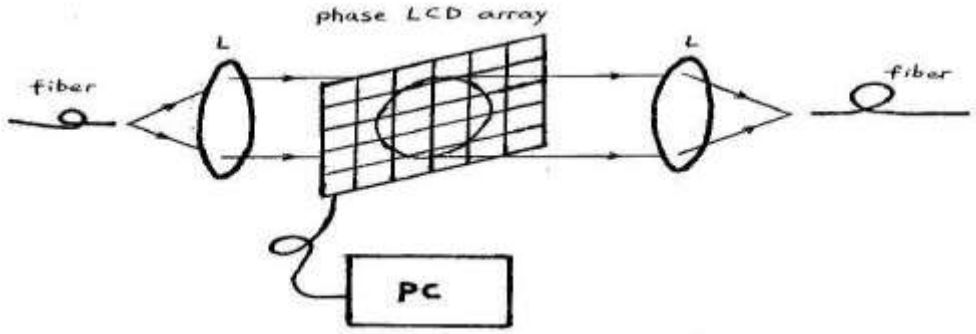

Fig. 1.1: Phase-LCD array based adaptive attenuator

6. LIQUID-CRYSTAL BASED FOSA WITHOUT MOVING PARTS

The LC FOSA that we previously proposed consists of a series of birefringent filters with different free spectral ranges (FSRs).

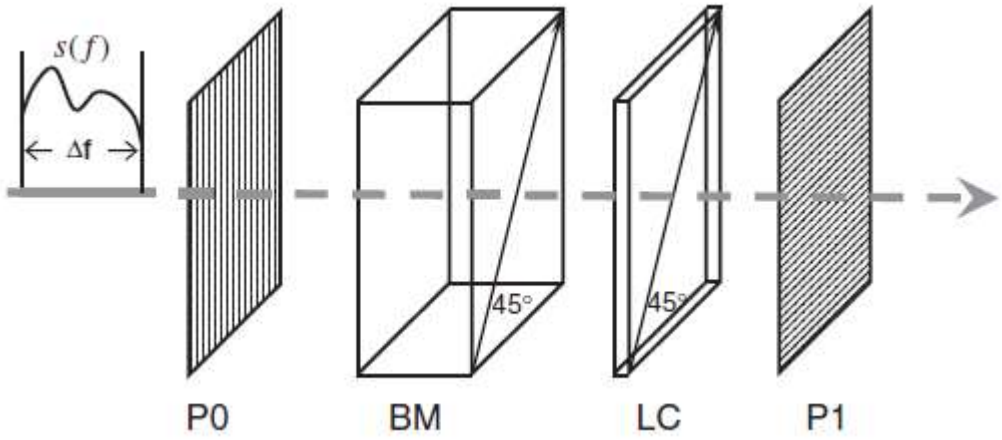

Fig.1.2: Schematic diagram of single stage in LC-controlled FOSA. P0 and P1 denote crossed polarizers, and BM is a 45-oriented birefringent material.

Three control LC cells are employed in each FOSA stage to modulate the transmittance of each filter. Although the three-cell design provides the possibility of realizing cascading one-dimensional system architecture, the precise control of these LC cells is complex and becomes more difficult in a multi-stage FOSA. To solve this problem, in this study, we demonstrate an improved and simplified design of a FOSA, as shown in Fig. 1.2. The new FOSA uses only one LC cell sandwiched between two crossed polarizers. The electronic control of the phase retardation of the cell is simplified considerably. In Fig. 1.2, P0 and P1 is two crossed polarizer's. Although parallel polarizers can also work, crossed polarizers are preferred because of their ease of alignment. BM represents a 45-oriented birefringent material that could be a crystal or a liquid crystal. An electrically controlled homogeneous LC cell is placed behind the BM. Its optical axis is parallel to that of the BM, as shown in Fig. 8, so that the total phase retardation of BM and LC is additive. In such a FOSA stage,

Incoming light becomes linearly polarized after passing through P0 and is decomposed into two equal orthogonally polarized components in BM and LC. These two polarizations components recombine at P1 to generate optical interference. Obviously, this is a typical birefringent filter with a transmission of $T(f)=Sin^2[(\Gamma+\Gamma_{LC})/2] = (1/2)[1-\cos(2\pi f/FSR + \Gamma_{LC})]$ where f is the light frequency and $\Gamma= 2\pi f/FSR$ and Γ_{LC} represent the phase retardation of the BM and LC cells, respectively. By tuning the applied voltage to the LC cell, LC directors are reoriented. As a result, Γ_{LC} changes and different transmission functions are obtained. For the FOSA application, the LC cell should be operated at 3 different retardation states, i.e.,

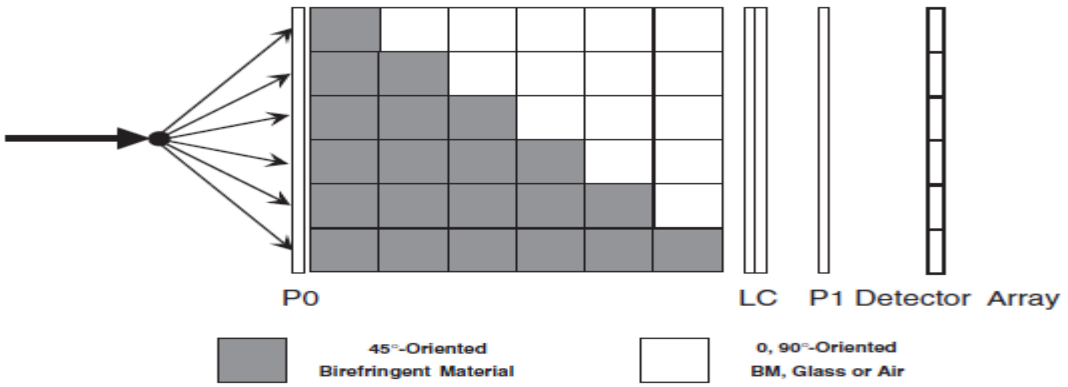

Fig.1. 3: System architecture of 6-stage LC-based FOSA.

Γ_{LC} = 2π, π/2 and , 3π/2 at which the corresponding light transmittances are I1, I2, and I3, respectively. It has been proven that the mth-order Fourier series coefficients of the input spectrum s(f) may be calculated from I1, I2, and I3 by virtually expanding s(f) with a frequency period of FP = m.FSR As a consequence, the input spectrum can be reproduced from its Fourier coefficients by employing sufficient stages with multiple FSRs. The whole FOSA system consists of a number of these stages that are packaged in parallel. Figure 1.3 shows the system architecture of such a FOSA. The input beam is separated into some channels with equal intensity by a 1 X N polarization independent beam splitter, which is generally a planar-lightwave-circuit-based device. Each channel with a collimated input beam corresponds to a birefringent filter stage. The gray blocks represent the 45^0- oriented birefringent materials, thus different stages will show different phase retardations. The white blocks could be 0^0 or 90^0oriented birefringent materials, optical glasses, or even just air which have no contribution to phase retardation. Because these birefringent filters are aligned parallel to each other, a single LC cell is sufficient for generating all the required phase states. Behind the polarizer P1, a photodetector array is placed to measure transmitted light intensity. Each detector pixel corresponds to a single FOSA channel so that an N-pixilated detector array is needed for an N-staged FOSA. Then the input spectrum can be reproduced with the Fourier coefficients computed from the detected light intensities in different pixels. There are two key parameters for the LC-controlled FOSA: the maximum measurable spectral range and the minimum spectral resolution. Because the Fourier series only gives a periodic function, the maximum measurable spectral range is thus less than FP, which is just the FSR of the first FOSA stage. FSR is determined by material birefringence and thickness, thus, it should be carefully chosen to match a specific application. For example, for a telecom-based FOSA, the FSR should be wider than an International Telecommunication Union (ITU) spectral band with a width of 5 THz.

The spectral resolution of a spectrometer could be generally described as $|\delta f/f = |\delta\lambda/\lambda| = \lambda/\Delta l$ Regardless of spectrometer type, where δf and δλ are the minimum distinguishable frequency and wavelength, respectively? Delta l is the largest optical path difference between interfered lights. In a LC FOSA, Delta l is the maximum optical retardation among all FOSA stages. Thus, the FOSA resolution can be δf = FP/N derived as To increase spectral resolution, more FOSA stages have to be used. These stages may be aligned in a two-dimensional matrix to maintain a compact device footprint. However, in a fiber-optic communications system, all the light sources and amplifiers used have slowly varying spectral shapes, such as an erbium-doped fiber amplifier or a semiconductor amplifier. A low-resolution FOSA with less than 10 stages should be enough for telecom applications. In addition to resolution, stage number N also affects the detected signal-to-noise ratio (SNR). The SNR is determined by the collected light intensity of each FOSA stage and the detector array's sensitivity. More stages may lower the SNR. A commercially available detector array has a responsivity of 0.95 A/W and a dark current of 0.03 nA. If only 1% power light is taped to a LC FOSA (<10 stages) for spectrum measurement, the total system light power should be higher than 0.063mW to ensure SNR > 30 dB. Here, the 50% power loss of the polarizers has been taken into account. The actual transmitted light power in a DWDM system is at the milliwatt level, which indicates that the LC FOSA is sufficiently sensitive for practical applications.

7. CONCLUSIONS

To prove the design principle, a prototype 6-stage FOSA device working at approximately λ= 1.55 μm telecom band is experimentally demonstrated. Quartz crystals of 5mm Thickness is used as birefringent materials. The FSR for a single quartz crystal is calculated to be 7.1 THz in the nearinfrared band. Although only one crystal is used for the first FOSA stage, the device dimension is determined by the sixth stage with 6 quartz crystals. An 8-um-thick LC cell was used for the experiments. The inner surfaces of the substrates are coated with thin polyimide layers in ant parallel rubbing directions, which introduce a homogeneous alignment of LC molecules. Then the cell was filled with a Merck E44 LC mixture through a capillary effect. To determine the operating voltages of this LC cell, voltage-dependent transmittance was measured between the two crossed polarizers. the LC used in the experiment is just a simple homogenously aligned cell. The transition time between different driving voltages is over 100 milliseconds, which is not very fast. To reduce response time, several approaches can be considered, for example, the use of a high figure-of merit LC, the improvement of the driving scheme, and the introduction of polymer networks into LC. We experimentally demonstrated a 6-stage FOSA without moving parts. Unlike normal spectrometers, the FOSA retrieves the spectrum's Fourier coefficients instead of performs the direct spectrum measurement by controlling the phase retardation of a LC phase modulator. The measured spectrum of an infrared source shows a reasonably good agreement with the real spectrum. Some possible approaches to improving the FOSA performance are also discussed.

8. REFERENCES

[1]. Ford, J.E.; Walker, J.A, Broadband Optical Networks and Technologies: An Emerging Reality/Optical MEMS/Smart Pixels/Organic Optics and Optoelectronics. 1998 IEEE/LEOS Summer Topical Meetin , 1998, pp I/9 -I10

[2]. Offrein, B.J.; Bona, G.L.; Germann, R.; Horst, F.; Salemink, H.W.M, LEOS '99. IEEE Lasers and Electro-Optics Society 1999 12th Annual Meeting , Volume: 2 , 1999, pp 547 -548 vol.2

[3]. Doerr, C.R.; Joyner, C.H.; Stulz, L.W, IEEE Photonics Technology Letters , Volume: 10 Issue: 10 , Oct. 1998, pp 1443 -1445

[4]. Mansell, Justin Dennis, "Micromachined Deformable Mirrors for Laser Wavefront Control", PhD thesis, Electrical Engineering Department, Stanford University, Feb, 2002, Chapter 4

[5]. T. G. Bifano, J. Perreault, R. Krishnamoorthy Mali, and M. N. Horenstein. "Microelectromechanical Deformable Mirrors", IEEE J. of Sel. Top. In Quan. Elec. **5**, 83-9, 1999.

[6]. M. A. Michalicek, N. Clark, J. H. Comtois, and H. K. Schriner. "Design and simulation of advanced surface micromachined micromirror devices for telescope adaptive optics applications", SPIE Vol. 3353, 805-815, 1998.

[7]. A. Ramamoorthy, *Thermotropic Liquid Crystals: Recent Advances*, (Springer, 2007).

[8]. G. Friedel, *Ann. Phys.*, 18, 273 1922.

[9]. A. D. Buckingham, G. P. Ceaser and M. B. Dun, "Addition of optically active compounds to nematic liquid crystals", *Chem. Phys. Lett.*, 3, 540-541, 1969.

[10]. H. S. Kitzerow, and C. Bahr, *Chirality in liquid crystals*, (Springer-Verlag,2001)

[11]. V. N. Tsvetkov, and G. M. Mikhailov, *Acta Physicochim*, U.R.S.S, 8, 77,1978.

[12]. S. K. Ghosh, "A model for orientational order in liquid crystals", *Il Nuovo Cimento D*, 4 (3), 229-244,1984.

[13]. D. Demus, J. Gooby, G. W. Gray, H.W. Spiess, and V. Vill, *Physical properties of liquid crystals*, (Wiley-VCH, 1999).

[14]. S. Singh, and D. A. Dunmar, *Liquid Crystals: fundamentals*, (World Scientific, 2002).

[15]. D. K. Yang, and S. T. Wu, *Fundamentals of Liquid crystal devices*, (JohnWiley & Sons, 2002).